Containment strategy for an epidemic based on fluctuations in the SIR model

Philip Bittihn¹ and Ramin Golestanian^{1,2}

¹Max Planck Institute for Dynamics and Self-Organization (MPIDS), 37077 Göttingen, Germany ²Rudolf Peierls Centre for Theoretical Physics, University of Oxford, Oxford OX1 3PU, United Kingdom (Dated: March 24, 2020)

A pandemic creates a challenging situation where governing authorities are faced with the complex decision of what the appropriate measures are given the existing information. Building on the key observation that the stochastic evolution of a process such as the spread of infection has a finite extinction probability even when it is expected to grow exponentially on average, we propose a strategy of containment that falls in between the relatively mild social distancing measures and the maximally restrictive lock-down strategies. Our proposed strategy involves partitioning the population into smaller isolated sub-populations within which, while social distancing is practised as much as possible to reduce the contact rate, a relatively normal lifestyle is maintained. As a rule of thumb, the optimal size of the sub-populations can be obtained by dividing the total population size by the best estimate of the number of infected individuals at the time of the implementation of this containment strategy.

a. Introduction.— In the midst of the spread of infection by the novel corona-virus, current political efforts are mainly aimed at reducing the rate of contact-based infection (by limiting social interactions and quarantining infected people, thus effectively removing them from the pool that can infect susceptibles). This is hoped to lead to an overall smaller peak in the infected fraction of the population. Typical responses by governments have started from relatively mild measures in the form of travel restrictions implemented between whole nations and shut down of major gatherings, and switched to extreme measures that limit the mobility of individuals to the confines of their homes. According to our analysis, which is based on the effect of fluctuations in the spread of infection, it is possible to propose an alternative scenario that introduces an intermediate level of restrictions and contains the spread of infection. Our scenario considers the very early stages of an epidemic when the spread is expected to grow exponentially on average. The key idea is that more stringent isolation of smaller sub-populations could make use of stochastic effects and increase the likelihood of a spontaneous end of infection chains in local communities via a process called extinction. We find that strict isolation at the level of sub-populations also has the advantage of leading to stochastic desynchronization of the epidemic bursts, such that not all sub-populations reach peak at the same time and the total peak number of infected individuals in the entire population is further reduced (see Figs. 1a and 1b).

There exists extensive prior work on the spread of infections through populations of various topological structure; see, e.g., Ref. [1] and the references therein. Data analysis on the trends of the recent epidemic spread has revealed heterogeneity in the degree of infectiousness of the virus [2] and in the phylogeny of the virus across different regions [3], and has been used to quantify the effectiveness of the containment measures [4, 5]. Evidence is also emerging on the role of stochasticity in the effectiveness of containment measures, as can be seen for example from the case of nearby cities for which implementation of similar measures led to drastically different trends [6]

We consider a population of N individuals with SIR (Susceptible S, Infected I, and Removed R (due to either recovery or death)) dynamics [7]

$$S + I \xrightarrow{b} I + I,$$
 (1a)

$$I \xrightarrow{k} R,$$
 (1b)

with infectious contact rate b and removal rate k. These rates are related to the basic reproduction number $R_0 =$ b/k, which is commonly used to quantify the intensity of an outbreak [1]. The population is subject to the total constraint N = S + I + R. This simple model has been used in many studies of disease spreading [1] but more sophisticated generalizations have also been developed [8, 9]. All numerical results shown below are obtained from stochastic simulations of Eq. (1) using the Gillespie algorithm [10].

c. Deterministic behaviour.— The dynamics results in the deterministic mean-field equations

$$\frac{\mathrm{d}I}{\mathrm{d}t} = \frac{b}{N} \, S \, I - k \, I,\tag{2a}$$

$$\frac{\mathrm{d}S}{\mathrm{d}t} = -\frac{b}{N} S I, \qquad (2b)$$

$$\frac{\mathrm{d}R}{\mathrm{d}t} = k I, \qquad (2c)$$

$$\frac{\mathrm{d}R}{\mathrm{d}t} = k\,I,\tag{2c}$$

which give rise to two regimes in the dynamics. During the initial regime I starts off from an initial value I_0 and rises exponentially, $\sim I_0 e^{(b-k)t}$, and saturates to some peak value I_{max} .

$$I_{\text{max}} = \gamma N, \tag{3}$$

where the maximum fraction of the infected population, $\gamma(b,k)$, is defined. Note that by definition, $0 < \gamma < 1$, and that it only depends on the ratio of the two rates, namely $\gamma(b,k) = \gamma(b/k)$. In the secondary regime when

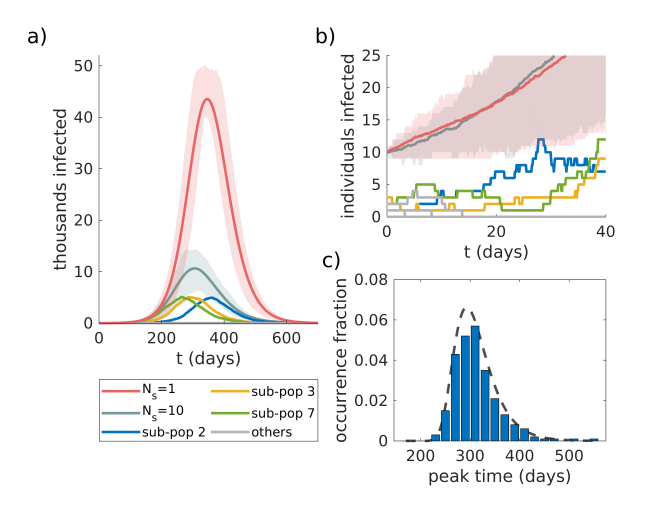


FIG. 1: Desynchronization of sub-populations. (a) Time course for a population of N = 1,000,000 with $I_0 = 10$ initially infected individuals for $N_s = 1$ large population (red) and a population split into $N_s = 10$ sub-populations (turquoise). Shading indicates $\pm 25\%$ confidence intervals across 100 simulations. Colour-coded sub-populations are shown from one such simulation for $N_s = 10$. Only three sub-populations experience a significant outbreak, and they are desynchronized. (b) Enlarged plot of the initial phase, during which 7 out of 10 sub-populations experience extinction, whereas the expectation value for both $N_s = 1$ and $N_s = 10$ rises exponentially. (c) Distribution of peak times in sub-populations for $N_s = 10$. Occurrence fraction indicates the fraction of sub-populations showing the corresponding peak time across all 100 simulations from (a). Note that this distribution is not normalized since a significant fraction of sub-populations experience extinction of the epidemic and therefore do not exhibit a peak. Dashed line indicates the analytical approximation from Eq. (12) with a uniform $n = I_0/N_s = 1$. b = 0.1, k = 0.07 for all simulations.

the recovery dynamics dominates, I decays to zero exponentially, as the number of susceptibles decreases below the value necessary to sustain spreading.

d. Small numbers.— Deterministic behaviour only applies if S and I are both large, particularly only after the number of infected people I has risen to appreciable levels. If I is still low, stochastic effects determine whether I will "take off" and develop exponential behaviour, even if b > k. During this phase we can assume that $S \approx N$ and that I follows a simple birth-death process with rates b for birth and k for death. From the theory of branching processes, it is well known that even an exponentially growing population that starts from an initial condition of I(0) = 1 has a finite extinction probability of

$$\mathcal{P}_0(t) = \frac{k}{b} \cdot \frac{e^{(b-k)t} - 1}{e^{(b-k)t} - k/b} \quad . \tag{4}$$

which asymptotically approaches k/b at long times [11]; see the derivation in Appendix A. This means that with probability $p_1^{\text{ext}} = k/b$ [12] the dynamics never enters

the exponentially growing deterministic regime, but decays back to zero due to number fluctuations. For two independent lineages in the same population, the extinction probability is therefore $p_2^{\rm ext}=(k/b)^2$, and, similarly, $p_n^{\rm ext}=(k/b)^n$, as long as the total population is large enough so that the lineages do not interfere with each other. If this assumption does not hold, the theoretical framework can be readily extended to adapt to the more general case.

e. Isolated sub-populations.— In a large population with N individuals, where the number of infected cases has already left the stochastic regime, the peak number of infected individuals will be $I_{\text{max}} = \gamma N$ (as defined in Eq. (3) above). In contrast, if the population is split up into N_s equal sub-populations, some sub-populations can experience extinction of the outbreak due to the low number of initially infected individuals. An example for populations of N = 1,000,000 individuals split into $N_s = 10$ sub-populations is shown in Figs. 1a and 1b, along with the expected dynamics of a single large population. Note that, on average, both the undivided large population and the sum of the smaller sub-populations initially exhibit an exponential growth in the number of infected individuals (Fig. 1b). The effect of the extinction events in some sub-populations is only seen later during the saturation phase.

To obtain an estimate for this effect, we add up the maximum numbers of infected individuals in the sub-populations. Each of these peaks is approximately $\gamma N/N_s$, but only if the infection does not stochastically become extinct during the initial stages. On average, the peak number in each case will be

$$I_{s,\text{max}}(n) = \gamma \frac{N}{N_c} \left(1 - p_n^{\text{ext}} \right) \tag{5}$$

where n indicates the number of initial infected individuals in the sub-population and $p_n^{\rm ext}$ is the probability that they go extinct without entering deterministic growth as discussed above. By following this *containment* strategy, the total peak number of the infected individuals in all the sub-populations is then

$$I_{\text{max}}^{\text{con}} = \sum_{n} g_n I_{s,\text{max}}(n), \tag{6}$$

where g_n is the number of sub-populations with n initially infected individuals. Note that

$$N_s = \sum_n g_n. (7)$$

Combining the above equations, we obtain

$$I_{\text{max}}^{\text{con}} = \gamma \frac{N}{N_s} \sum_{n} \left(1 - p_n^{\text{ext}} \right) g_n = \gamma N \left[1 - \frac{\sum_{n} g_n (k/b)^n}{\sum_{n} g_n} \right].$$
(8)

The above result manifestly shows that

$$\gamma^{\rm con} \equiv \frac{I_{\rm max}^{\rm con}}{N} < \gamma, \tag{9}$$

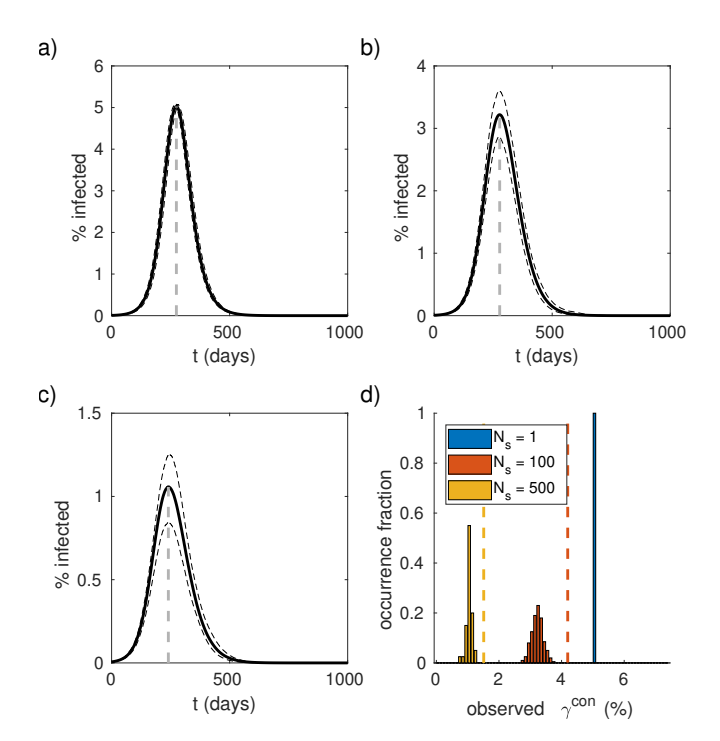


FIG. 2: Epidemics for different sizes of sub-populations. Time course (solid line) and 2.5/97.5 percentiles (dashed lines) for a total population of N=8,000,000 individuals and 500 initially infected people. (a) $N_s=1$ (20 individual simulations). (b) $N_s=100$ with randomly distributed infected individuals (200 individual simulations). (c) $N_s=500$ with randomly distributed infected individuals (40 individual simulations). (d) Distribution of the observed peak percentage of infected individuals for the same three ways of population splitting. Occurrence fraction indicates the fraction of simulations exhibiting the corresponding $\gamma^{\rm con}$. The dashed vertical lines indicate the value expected from Eq. (8) assuming a uniform distribution of individuals across sub-populations. Occurrence fraction indicates the fraction of simulations exhibiting the corresponding $\gamma^{\rm con}$. b=0.1, k=0.07 for all simulations.

holds. Note that the simple summation of the individual maxima neglects the possible desynchronization between sub-populations (see below for more details and a comparison of Eq. (8) with simulations in Figs. 2d and 3b).

For example, for the ideal case where each subpopulation only contains at most one infected individual, we will have

$$I_{\text{max}}^{\text{con}} = \gamma \, \frac{N}{N_s} \left(1 - \frac{k}{b} \right) I_0, \tag{10}$$

where $g_1 = I_0$ is the total number of initially infected individuals in the large population (for this to make sense, $N_s \geq I_0$ is required). Comparing this with the peak value in Eq. (3), which corresponds to the case where the population was not split up, we find that the peak number of infected (and thus proportionally the hospital beds required) can be reduced by a factor of

$$\frac{I_{\text{max}}^{\text{con}}}{I_{\text{max}}} = \frac{\gamma^{\text{con}}}{\gamma} = \frac{I_0}{N_s} \left(1 - \frac{k}{b} \right), \tag{11}$$

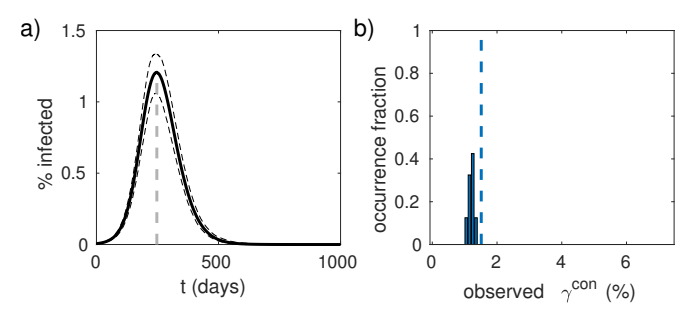


FIG. 3: Uniform distribution of infected individuals. (a) Time course (solid line) and 2.5/97.5 percentiles (dashed lines) for a total population of N=8,000,000 individuals, $N_s=500$ subpopulations and 500 initially infected people (40 individual simulations). Instead of randomly distributing the 500 infected individuals across the sub-populations as in Fig. 2, exactly one infected was placed in each sub-population. (b) Distribution of the observed peak percentage of infected individuals. Occurrence fraction indicates the fraction of simulations exhibiting the corresponding $\gamma^{\rm con}$. The dashed vertical line indicates the value expected from Eq. (8) assuming the same uniform distribution of individuals across sub-populations. $b=0.1,\ k=0.07.$

in the optimal case, which can be decreased by increasing the number of sub-populations N_s and bringing b closer to k. Note that this is in addition to the decrease in the deterministic peak fraction γ of infected, which naturally results when b becomes closer to k.

The independent summation of maxima in different sub-populations is a conservative estimate, since fluctuations can lead to stochastic desynchronization and thus to a further reduction of the peak value. The distribution of peak times in the sub-populations from the previous example is shown in Fig. 1c. The temporal shift between the different sub-populations can be attributed entirely to stochastic fluctuations in the initial phase of the dynamics. Assuming that this time shift accumulates while the dynamics can still be modeled as a pure birth-death process without saturation effects, we can derive the probability distribution for the deviation from the mean peak time $\Delta t_{\rm peak} \equiv t_{\rm peak} - \langle t_{\rm peak} \rangle$ as

$$P(\Delta t_{\text{peak}}) = k(1 - k/b)[1 - (k/b)^n]$$

$$\times \exp\left(-(b - k)(\bar{\tau} + \Delta t_{\text{peak}}) - \frac{k}{b}e^{-(b - k)(\bar{\tau} + \Delta t_{\text{peak}})}\right),$$
(12)

where n is the initial number of infected individuals in the population and $\bar{\tau} = \ln{(\gamma k/b)}/(b-k)$ with γ being the exponential of the Euler constant (see Appendix B for details). This result is in excellent agreement with the measured distributions (see dashed lines in Fig. 1c and Fig. 4).

f. Discussion.— Standard strategies to contain epidemic spreads are typically aimed at reducing b (by limiting social interactions and quarantining infected people), which leads to an overall decrease in γ . While

travel restrictions implemented between whole nations (and also between individual federal states) are the first large scale methods used for containment, according to the above analysis more stringent isolation of smaller subpopulations could make use of stochastic effects and increase the likelihood of a spontaneous end of infection chains in local communities. This would reduce the overall peak number of infected people (and therefore strain on the healthcare system) by an additional factor of up to $I_0/N_s \cdot (1-k/b)$ when $I_0/N_s < 1$, even if efforts of reducing b below k are not effective and b > k remains. One contribution comes from the communities which have no initially infected people and are now protected (I_0/N_s) , while another contribution comes from the possibility that an infection chain in the local community stochastically ends due to fluctuations (k/b). Stochastic desynchronization would further reduce the peak, since not all sub-populations reach peak values at the same time.

We consider as an example a region with a population of about 8,000,000 and 500 infected individuals $(I_0/N \sim 6 \cdot 10^{-5})$. Parameter estimates for the unconstrained evolution of the recent epidemic outbreak vary widely [2, 4, 5]. We assume initial parameters of b = 0.3and k = 0.07, corresponding to a basic reproduction number of $R_0 = b/k \approx 4.3$ and a removal time of $1/k \approx 14$ days, which are on the same order as estimates for other simple epidemiological models [2, 4] and yield a realistic growth factor of $e^{b-k} = 1.26$ per day in the early stages of the epidemic. Let us further assume that drastic measures, but without explicit confinement to homes, can improve the parameters of the epidemic to b = 0.1 and k = 0.07, but not enough to reduce b below k, which would prevent spreading altogether. If this population is allowed to mix homogeneously, the dynamics will evolve according the deterministic prediction with a peak around 5% (400,000 people) infected individuals (Figs. 2a and 2d).

If instead, the population is split up into 100 subpopulations of 80,000 people and the 500 infected people are distributed randomly across those 100 subpopulations, the peak of infected population decreases to around 3% (260,000 people) on average (Figs. 2b and 2d). Isolating even smaller communities from their surroundings (500 sub-populations of 16,000 people) leads to a further reduction of the peak to around 1% (85,000 people) on average (Figs. 2c and 2d). This is comparable (or even slightly lower) than the case where the 500 infected individuals are not distributed randomly across the 500 sub-populations, but each sub-population contains exactly one infected individual. In this case (Fig. 3), there are no sub-populations with initially zero infected individuals. This implies that the reduction in peak value compared to the large homogeneous population is strictly due to extinction, which also means that the remaining deviation from the prediction of Eq. (8) is probably due to desynchronization. The desynchronization for the three different ways of splitting

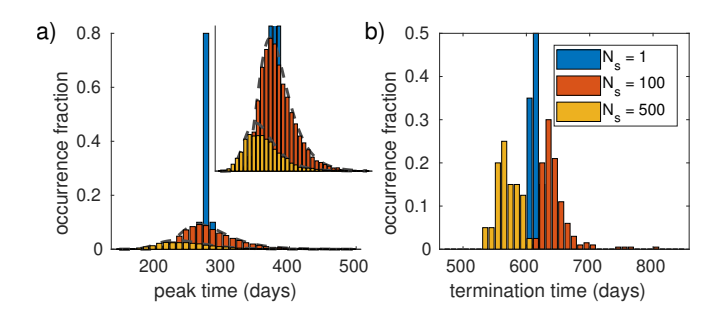


FIG. 4: Peak and termination time distributions. (a) Distribution of peak times for the three cases shown in Fig. 2, with a total population of N = 8,000,000 individuals and different N_s with 500 initially infected people. Occurrence fraction indicates the fraction of sub-populations showing the corresponding peak time across all simulations for the corresponding parameters. Note that these distributions are not normalized since a significant fraction of sub-populations experience extinction of the epidemic and therefore do not exhibit a peak. Inset provides an enlarged view of the two smaller distributions. Dashed lines indicate the analytical approximation from Eq. (12), assuming a uniform $n = I_0/N_s$ for each case. (b) Distribution of termination times for the same three cases. Termination time is defined as the time when the number of infected individuals drops below the initial number in the total population.

up the population shown in Fig. 2 is quantified in Fig. 4a, which shows a broadening of the peak time distribution owing to increased stochasticity. Note that there is also a subtle, non-monotonic effect on the termination time of the epidemic, whose distribution also tends to become broader when the population is split up (Fig. 4b).

In summary, even without complete lock-down and without achieving b < k, isolating smaller communities can significantly reduce the peak number of infected individuals of an epidemic outbreak. While this is obvious even from a deterministic standpoint in the case where many regions initially contain no infected individuals, our analysis shows that this advantage persists due to stochastic extinction events even if this is not the case, as long as $I_0/N_s \sim 1$. Due to the exponential dependence of the extinction probability on n (see Eq. (8)) it is important to obtain a conservative estimate for I_0 , for example by adjusting the number of reported cases by an appropriate factor related to the detection probability. Naturally, such isolation will also automatically lead to a further reduction in b, so that the reduction will be even greater in practice. In addition, given the available data about the geographic distribution of infections, it should be possible to isolate the "right" communities and adjust their size much more intelligently than we have done here (where the infected individuals were distributed randomly or uniformly across sub-populations). This should further increase the likelihood of stochastic termination of the epidemic in many small communities (even if there are undetected cases), and should also allow

for practical considerations and compromises regarding access restrictions to certain areas. Note that the additional desynchronization effect would also allow non-peak regions to provide medical support and hospital space to peak regions, further improving the management of the epidemic. Of course, this approach does not preclude the activation of more drastic individual confinement measures as a last resort in regions beginning to show deterministic exponential behaviour, while still sparing the majority of regions from them.

Bodenschatz, Wolfgang Brck, Hugues Chaté, Ragnar Fleischmenan, Tim Friede, Theo Geisel, Helmut Grubmller, Reinhard Jahn, Benoit Mahault, Viola Priesemann, Thomas Richter, Simone Scheithauer, Martin Siess, Andrej Vilfan, Michael Wilczek. We are indebted to Ramin Yahyapour for bringing Ref. [6] to our attention. The research was supported by the Max-Planck-Gesellschaft.

Acknowledgments

We have benefited from discussions with Jaime Agudo-Canalejo, Amir Bahrami, Heike Bickeboeller, Eberhard

- R. Pastor-Satorras, C. Castellano, P. Van Mieghem, and A. Vespignani, Rev. Mod. Phys. 87, 925 (2015).
- [2] T. Zhou, Q. Liu, Z. Yang, J. Liao, K. Yang, W. Bai, X. L, and W. Zhang, arXiv:2001.10530.
- [3] T. Matsuda, H. Suzuki, and N. Ogata, arXiv:2002.08802.
- [4] D. Fanelli and F. Piazza, arXiv:2003.06031.
- [5] P. Castorina, A. Iorio, and D. Lanteri, arXiv:2003.00507.
- [6] J. Beam Dowd, V. Rotondi, L. Adriano, D.M. Brazel, P. Block, X. Ding, Y. Liu, M.C. Mills, medRxiv (doi: https://doi.org/10.1101/2020.03.15.20036293).
- [7] W. O. Kermack and A. G. McKendrick, Proc. R. Soc. A 115, 700-721 (1927).
- [8] L. Tian, X. Li, F. Qi, Q.-Y. Tang, V. Tang, J. Liu, X. Cheng, X. Li, Y. Shi, H. Liu, and L.-H. Tang, arXiv:2003.07353.
- [9] K. Wu, D. Darcet, Q. Wang, and D. Sornette, arXiv:2003.05681.
- [10] D.T. Gillespie, J. Phys. Chem. 81, 2340-2361 (1977).
- [11] J. R. Norris, *Markov Chains* (Cambridge University Press, Cambridge, 1997).
- [12] Note that for simplicity of the presentation we are using the long time limit of the extinction probability to define p_1^{ext} rather than $\mathcal{P}_0(t)$ evaluated at a relevant time scale.
- [13] M.M. Desai and D.S. Fisher, Genetics 176, 1759 (2007).

Appendix A: Exact solution of the birth-death process

Consider a population of the infected individuals I that can undergo the following two processes:

$$I \xrightarrow{b} I + I, \qquad I \xrightarrow{k} \emptyset, \tag{A1}$$

i.e., each I can give birth to another I with rate b, or, it can die with rate k, at any time. Ignoring the stochasticity, the average behaviour of the system is described by exponential birth and death. The population $\bar{n}(t)$ can be determined as follows:

$$\frac{\mathrm{d}\bar{n}(t)}{\mathrm{d}t} = (b-k)\bar{n}(t) \quad \Rightarrow \quad \bar{n}(t) = e^{(b-k)t}, \tag{A2}$$

where we have assumed that the initial size of the population is one. As this is a one-step process, the probability of finding n copies of I in the sample at time t satisfies the following Master equation

$$\frac{\mathrm{d}\mathcal{P}_n(t)}{\mathrm{d}t} = k(n+1) \,\mathcal{P}_{n+1}(t) + b(n-1) \,\mathcal{P}_{n-1}(t) - (k+b) \,n \,\mathcal{P}_n(t),\tag{A3}$$

The factor of n is needed because the birth or death could happen to anyone. Equation (A3) can be solved by an ansatz of the form $\mathcal{P}_n \sim f^n$ for $n \geq 1$, which together with the initial condition $\mathcal{P}_n(0) = \delta_{n,1}$ gives us the solution as

$$\mathcal{P}_n(t) = \frac{\bar{n}(1 - k/b)^2}{(\bar{n} - 1)(\bar{n} - k/b)} \left(\frac{\bar{n} - 1}{\bar{n} - k/b}\right)^n. \tag{A4}$$

The distribution can be used to calculate the first two moments

$$\langle n(t) \rangle = \sum_{n=0}^{\infty} n \mathcal{P}_n(t) = \bar{n}(t) = e^{(b-k)t},$$
 (A5)

$$\Delta n^2 = \left\langle \left[n - \left\langle n \right\rangle \right]^2 \right\rangle = \left(\frac{b+k}{b-k} \right) e^{(b-k)t} \left[e^{(b-k)t} - 1 \right], \tag{A6}$$

which reveal more interesting features about the system. First, it is reassuring that the average population size behaves according to the mean-field description above that predicted exponential growth or decay. A quantity of interest is

$$\frac{\Delta n^2}{\bar{n}} = \left(\frac{b+k}{b-k}\right) \left[e^{(b-k)t} - 1\right],\tag{A7}$$

which probes whether number fluctuations follow a characteristic Poisson behaviour. In the long time limit, we have

$$\frac{\Delta n^2}{\bar{n}} = \begin{cases} \infty & ; \quad b > k, \\ \frac{k+b}{k-b} & ; \quad b < k, \end{cases}$$
 (A8)

which shows that while a decaying population that corresponds to b < k has a Poisson behaviour, a growing population corresponding to b > k has giant number fluctuations, which can be characterized via

$$\frac{\Delta n}{\bar{n}} = \sqrt{\frac{b+k}{b-k}} \sqrt{1 - e^{-(b-k)t}},\tag{A9}$$

which leads to

$$\frac{\Delta n}{\bar{n}} = \sqrt{\frac{b+k}{b-k}},\tag{A10}$$

in the long time limit. In other words, the fluctuations scale with the average population size when b > k, and with the square root of the average population size when b < k.

The above solution allows us to calculate the extinction probability of the population $\mathcal{P}_0(t)$, which is an absorbing state. We find

$$\mathcal{P}_0(t) = 1 - \sum_{n=1}^{\infty} \mathcal{P}_n(t) = \frac{k}{b} \cdot \frac{e^{(b-k)t} - 1}{e^{(b-k)t} - k/b}.$$
 (A11)

which is a very interesting result. When k > b, $\bar{n} \to 0$ at long times, and we obtain $\mathcal{P}_0 = 1$. It is no surprise that extinction at long times is a certainty when the death rate is larger than the birth rate. However, when k < b, $\bar{n} \to \infty$ at long times, and we obtain $\mathcal{P}_0 = k/b$; a result that is in contradiction with the prediction of the average behaviour of the system, which is exponential growth. So, number fluctuations could completely annihilate an exponentially growing population.

Appendix B: Analytical approximation of the relative peak time distribution

The fact that the early phase of the dynamics in the SIR model (when $S \approx N$ and I is small) corresponds to a simple birth-death process also allows us to obtain an analytical estimate for the peak time distributions of the sub-populations. This can be readily adapted from a similar calculation performed on an equivalent problem in evolution, where the dynamics of a small mutant sub-population with a given selective advantage can likewise be understood as a birth-death branching process

[13], for which the transition from the initial stochastic regime where extinction is still possible to the deterministic regime of exponential growth corresponds to the establishment of the mutation in the population (which precedes fixation).

We obtain an approximation for the establishment time distribution of the disease in a sub-population as

$$P_{\text{SIR}}^{\text{est}}(\tau) = k \left(1 - k/b \right) \exp\left(-(b - k)\tau - \frac{k}{b} e^{-(b - k)\tau} \right), \tag{B1}$$

where we have corrected for an additional minus sign missing from Ref. [13]. The variation in the timing of the later deterministic dynamics is due entirely to fluctuations in this initial stochastic phase. To compare this analytical approximation with our simulation results for the peak time in the main text, we plot the non-normalized, unconditional distribution

$$P(t_{\text{peak}}) = [1 - (k/b)^n] P_{\text{SIR}}^{\text{est}} \left(t_{\text{peak}} + \bar{\tau} - \langle t_{\text{peak}} \rangle \right), \text{ (B2)}$$

which is diminished by a factor $[1 - (k/b)^n]$ (from Eq. (B1)) accounting for the probability of extinction in a population with initially n infected individuals, and has its mean shifted to the measured mean peak time $\langle t_{\text{peak}} \rangle$. Here

$$\bar{\tau} \equiv \langle \tau \rangle = \frac{1}{b-k} \ln \left(\gamma \, \frac{k}{b} \right),$$
 (B3)

where $\gamma=1.7810724\cdots$ is the exponential of Euler's constant.

We note that simply shifting the mean of the distribution is justified because the dynamics is predominantly identical in different sub-populations once they are in the deterministic regime, while only lagging by a random time span τ . This simple argument depends on the assumption that stochastic fluctuations can be ignored before deviations from exponential behaviour (i.e. saturation effects) have to be considered for the deterministic dynamics. This is true for the scenarios we consider in the SIR model, since our sub-populations still consist of thousands of individuals and we are explicitly focusing on cases where b is not arbitrarily close to k.